Simultaneous fabrication of PDMS through-holes for three-dimensional microfluidic applications

Bobak Mosadegh,[a] Mayank Agarwal,[a] Yu-suke Torisawa[a] and Shuichi Takayama*[ab]

Received 24th February 2010, Accepted 27th April 2010
DOI: 10.1039/c003590d

Here we describe a simple yet efficient approach to making through-holes in a bound polydimethylsiloxane membrane for use in 3D microfluidic applications. Localized tearing of an elastomeric membrane is achieved by ripping an elastomeric stamp that is bound to the membrane by posts at desired regions. The tears in the membrane are confined by the underlying channel architecture of the substrate to which the membrane is bound. By varying the membrane thickness and channel dimensions, holes of different sizes can be obtained. This high-throughput method of generating through-holes will enable the design of complex microfluidic devices that require crossing of channel networks.

Introduction

Development of efficient fabrication techniques is an important area of research since it enables widespread use of microfluidic devices for many different applications.[1–3] The added versatility of three-dimensional microfluidics has been hindered by the inability to efficiently integrate through-holes into polydimethylsiloxane (PDMS) membranes used in multi-layer soft lithography. Through-holes provide passages between layers of a device enabling complex paths to bypass each other, which allows for the design of intricate devices. This type of 3D plumbing has been shown to be useful for a myriad of applications including combinatorial mixing of fluids,[4] integrated pneumatic valve devices,[5] and passive auto-regulating components.[6–8]

There are currently several low-cost methods to generate through-holes in thin PDMS membranes. One of the simplest is to manually punch out each hole using a small gauge needle or biopsy punch as done for access holes for most microfluidic devices.[9] Although simple and effective, this method is tedious and time-consuming, particularly for devices requiring many holes and is limited to through-hole sizes on the order of hundreds of microns. As an alternative, perforated membranes can be fabricated using an SU-8 mold pressed against a hard-surface during curing of the membranes or spinning PDMS lower than the tallest feature height.[6,10] However, often thin films of PDMS are cured over the SU-8 feature requiring manual removal, making this approach inefficient for high-throughput fabrication, particularly for thick membranes (>30 μm).[5] Recently there have been simple methods to eliminate the presence of the thin film by blowing with an air gun, but this requires manual aiming on each hole and provides additional design restrictions on the spacing between holes, which limits the density able to be integrated into a single device.[11] Selective ripping of PDMS substrates has been previously shown as a simple way to fabricate features on a flat substrate at both the microscale and nanoscale.[12,13] Use of decal transfer microlithography also provides a means to form through-holes by selective release of a micropatterned membrane, however the membrane is more effectively used for stencils than for 3D microfluidic applications since the top surface of the membrane is coated with non-stick material that inhibits proper bonding to another PDMS layer, and there is formation of a meniscus around each feature that will result in bonding gaps between layers.[12] Using this concept of selective ripping of PDMS, we have developed an efficient single-step method to simultaneously fabricate a large number of through-holes in a bound PDMS membrane using conventional microfluidic tools.

Experimental

All PDMS materials were made from PDMS prepolymer and curing agent (Sylgard 184, Dow Corning Co., Midland, MI) at a 10 : 1 ratio. PDMS stamps were molded against master molds made by standard photolithography using the negative-photoresist SU-8 (MicroChem Co., Newton, MA). The master molds were silanized in a desiccator for two hours (United Chemical Tech., Bristol, PA). The heights of all features are 80 μm. The PDMS molds were cured in a 120 °C oven for at least 30 min. PDMS membranes were made by spin-coating a PDMS layer on a silanized glass slide and then curing in a 120 °C oven for at least 30 min. For the characterization experiments, PDMS layers were oxidized/bonded together using a plasma etcher in air (SPI Plasma-Prep II, Structure Probe, Inc., West Chester, PA) for 30 s. An unnecessary but useful step prior to bonding of the post stamp is microcontact printing of uncured PDMS oligomers on areas between post regions to render the surface hydrophobic.[14] This step has been seen to minimize non-specific binding of the post stamp to undesired regions of the membrane. For the 3D microfluidic device demo, the stamp was bonded to the membrane using PDMS glue (mixture of 1 part toluene to 2 parts PDMS) spin coated on a glass slide at 1500 rpm for 30 s. The glue was cured in a 120 °C oven for 20 min. Shrinkage of PDMS was noticed but did not cause any alignment issues since the stamp

[a]*Department of Biomedical Engineering, University of Michigan, 2200 Bonisteel Blvd, Ann Arbor, Michigan, 48109-2099, USA. E-mail: takayama@umich.edu*
[b]*Macromolecular Science and Engineering Center, University of Michigan, 2300 Hayward St., Ann Arbor, Michigan, 48109, USA*

for tearing and the device structures were all prepared simultaneously with the same batch of PDMS under the same curing conditions.

Results and discussion

Three-dimensional microfluidic devices typically consist of two thick PDMS layers that sandwich a thin PDMS membrane. To generate through-holes in the thin PDMS membrane at particular locations of the channel network, a stamp is fabricated that has posts that spatially correspond to those locations. The channel network is first bound to a thin PDMS membrane (Fig. 1A, B) and subsequently the stamp is aligned and bonded to the membrane (Fig. 1C). Alignment of the stamp was performed manually under a stereoscope, although jigs can be constructed to provide additional accuracy, if necessary. There are several methods that can be used to bond the stamp to the membrane, depending on the accessibility of equipment.[15] Typical methods are oxygen plasma, corona discharge, and PDMS glue. Oxygen plasma allows for quick bonding but requires a low-vacuum machine which is bulky and expensive. A portable hand-held corona discharge (which is relatively inexpensive) can be used but typically gives less consistent results due to the uneven exposure to the device. PDMS glue is also an inexpensive alternative and provides some degree of error with alignment since bonding occurs only after baking, however the glue itself can spread limiting the resolution to which holes can be made. After the stamp has bonded, the stamp is simply torn from the membrane by hand and the membrane tears at the locations of the posts and the tear is localized by the channel's underlying features. It is best to tear the stamp orthogonal to the membrane surface in order to minimize tearing along channel features. Shown in Fig. 1, 2, and 3 are through-holes made at the intersection of two channels in order to demonstrate that this method is effective at creating localized through-holes in arbitrary channel configurations, however, through-holes can also be made at channel dead-ends as demonstrated in Fig. 4.

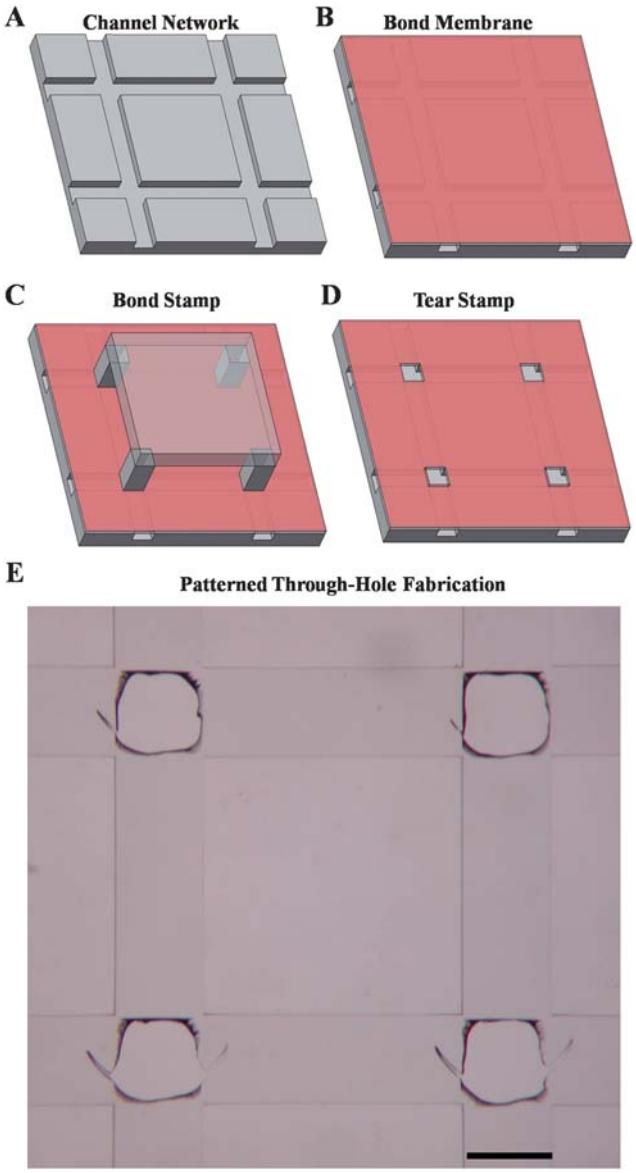

Fig. 1 Scheme for fabricating holes. (A) Representative channel network. (B) A PDMS membrane is bonded to the channel network. (C) A stamp with posts is bonded at desired locations. (D) Pull of stamp to tear holes at bonded locations. (E) Image of channel network shown in A. Scale Bar: 480 μm.

In order to keep tears confined in a desired location, the membrane must tear across the channel feature. Normally this occurs due to equal strain being imposed on the membrane from all directions (as the post is being pulled orthogonally from the substrate) and the anchoring of the bonded regions of the membrane, however in some cases the membrane can tear along the channel features before tearing across the channel producing a larger than intended hole (Fig. 2A). To circumvent this, "narrowed" channel geometries can be used in order to ensure that the membrane will tear inside a desired location (noted as the square location) (Fig. 2B).

To characterize this method, we constructed a channel geometry that corresponded to a stamp that would make an array of holes with varying dimensions of the underlying "square" (intersection of two channels features), narrowed features, and post (Fig. 3A). Two "square" sizes, 480 μm and 240 μm, with narrowing and post sizes that were either equal, half, or a fourth in size were tested. For each of these conditions, there were three replica holes on a single substrate. It can be seen in Fig. 3B that when a post of a smaller geometry was used on a larger square size, an overhanging membrane was left behind. This type of hole fabrication can be advantageous for three-dimensional components such as check-valves.[16] Typical images for both a 30 μm and 100 μm membrane are shown (Fig. 3C, D) with detailed results given in Table 1. Overall, it can be seen that smaller holes are more easily generated in thinner membranes; however, holes can be made in thick membranes (≥100 μm) with larger square sizes. For failed geometries, gashes were left in the membrane instead of through-holes which can also be advantageous for fabricating features of varying heights, which typically requires many steps when done using conventional photolithography. The "narrowed" geometries seem to only be necessary for large feature sizes (≥480 μm) to confine holes. It can also be seen that the narrowed geometries affect hole sizes for thicker

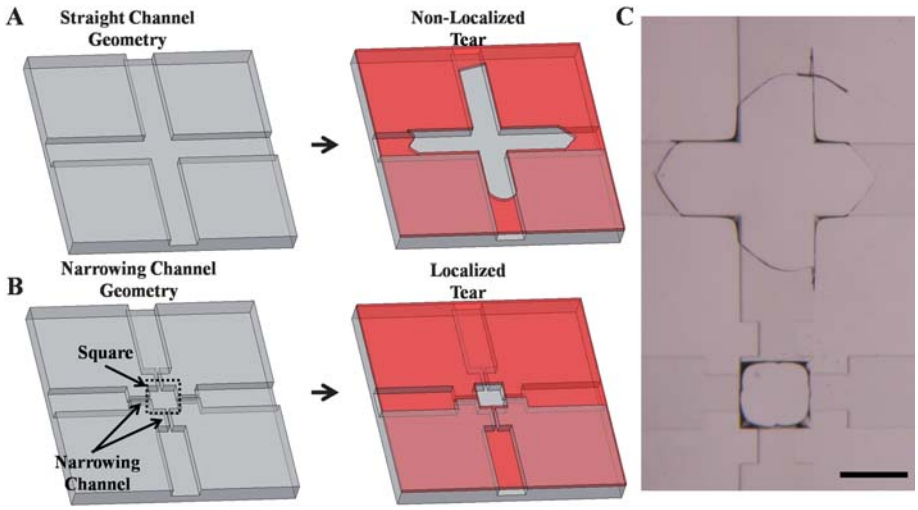

Fig. 2 Narrowed geometry confines tear. Straight channel (A) and narrowed channel (B) geometries can yield disparate hole sizes. (C) Respective image of channel networks shown in A. Scale Bar: 480 μm.

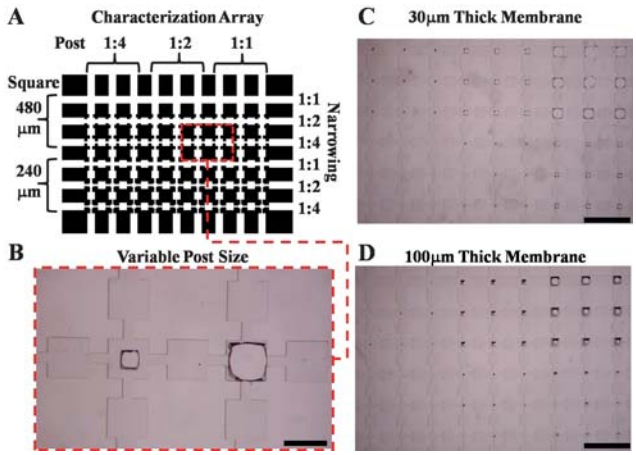

Fig. 3 Geometry characterization. (A) Diagram channel networks to characterize efficiency of different geometries. (B) Image if two different post sizes on the same square size demonstrating different hole sizes can be obtained. Scale Bar: 480 μm. (C–D) Images of characterization array for 30 μm (C) and 100 μm (D) membrane thickness. Scale Bar: 2 mm.

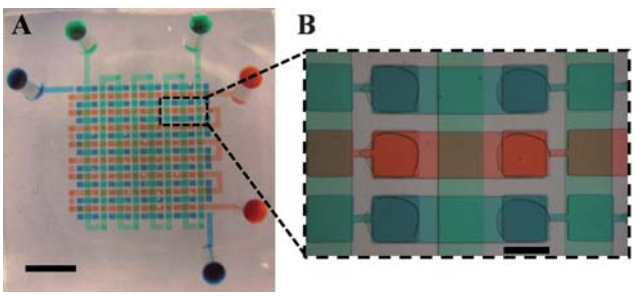

Fig. 4 Large-scale hole fabrication for 3D network. (A) Network of meandering microfluidic channels that cross in three-dimensions containing three separate solutions. Scale Bar: 3 mm. (B) Close-up image of holes and under-passing blue and red channels. Scale Bar: 480 μm.

membranes, decreasing the hole size with decreasing narrowed size. Although the smallest holes presented here were ~40 μm diameter, we believe smaller holes can be achieved with thinner membranes and/or smaller posts. Another factor that will influence the efficacy of this method is the alignment of the stamp to the bound membrane. This step becomes more difficult as feature sizes become smaller and over a larger total area that can't be viewed at once under a stereoscope. In cases where manual alignment is difficult, a jig that holds the stamp and can be precisely maneuvered will be useful.[17]

As a demonstration of the effectiveness of this method, we fabricated a microfluidic device with three sets of meandering channels that overlap each other in three-dimensions (Fig. 4A). This device consists of 152 holes that were all fabricated simultaneously in a 30 μm thick membrane using the described method. For this particular device, the stamp was bonded using the PDMS glue method which successfully generated localized holes with no special bonding equipment (Fig. 4B). This was done by spin coating a PDMS/toluene mixture on a glass slide and then microcontact printing the stamp.[18,19] The stamp was then aligned to the membrane-channel composite and bonded by thermal baking. Previous methods have typically only demonstrated devices with an order of magnitude less the number of through-holes[5,11] presented here.

Summary and outlook

We have described a low-cost method to efficiently fabricate through-holes simultaneously in large-scale. By altering channel and membrane dimensions, holes of varying sizes on a single substrate can be generated. While other methods are efficient at generating holes of very small dimensions (both in cross-section and height), the described method is uniquely suited for generating holes in thick membranes with relatively large cross-sectional areas. We believe that by overcoming the practical limitation of producing relatively large though-holes efficiently, this method will enable the development of intricate 3D devices that can facilitate objects such as cells and microbeads. In addition, embedded components that regulate fluid flow on-chip have been developed and these devices require through-holes to navigate fluids to both layers of the device to actuate the

Table 1 Geometry characterization data. Percentages are averages of ten or more holes that were successfully made (complete through-hole and confined to desired location) for each condition. Hole sizes (diameter in microns of opening at the bottom surface of the membrane) are only for successfully made holes except for those conditions which yielded no successful holes in which case the diameter of the gash (at the top surface of the membrane) is provided

		Post: Square					
		Membrane: 30 μm			Membrane: 100 μm		
Square size	Narrowing	1 : 4	1 : 2	1 : 1	1 : 4	1 : 2	1 : 1
480 μm	480 μm	60% 25.3 ± 3.6	100% 182.3 ± 16.1	80% 377.3 ± 48.7	0% 97.2 ± 25.8	33% 55.7 ± 16.1	100% 277.9 ± 24.5
	240 μm	73% 37.2 ± 6.8	100% 199.5 ± 11.7	100% 370.1 ± 48.1	0% 93.6 ± 19.7	1% 238.33 ± 1.7	100% 193.2 ± 48.2
	120 μm	80% 37.7 ± 5.2	93% 194.1 ± 3.3	100% 375.8 ± 32.9	0% 83.9 ± 15.1	2% 226.7 ± 14.4	100% 147.9 ± 25.8
240 μm	240 μm	0% 41.6 ± 9.5	67% 39.8 ± 1.86	100% 136.8 ± 36.0	0% 41.0 ± 9.3	0% 82.1 ± 15.0	0% 170.4 ± 29.8
	120 μm	0% 38.5 ± 16.3	47% 35.0 ± 4.7	93% 143.4 ± 20.9	0% 45.1 ± 10.5	0% 72.3 ± 38.4	0% 119.5 ± 39.4
	65 μm	0% 41.5 ± 10.9	53% 40.3 ± 5.8	80% 114.1 ± 29.2	0% 40.9 ± 10.4	0% 71.8 ± 26.0	0% 144.0 ± 12.4

sandwiched membrane.[6–8] Therefore high-thoughput fabrication methods like the one described in this paper will be essential for the development of more intricate designs.

Acknowledgements

We thank the NIH (HL-084370) for financial support. B.M. acknowledges funding TEAM training grant supported by National Institute for Dental and Craniofacial Research.

References

1 J. West, M. Becker, S. Tombrink and A. Manz, *Anal. Chem.*, 2008, **80**, 4403–4419.
2 A. J. deMello, *Nature*, 2006, **442**, 394–402.
3 D. Janasek, J. Franzke and A. Manz, *Nature*, 2006, **442**, 374–380.
4 C. Neils, Z. Tyree, B. Finlayson and A. Folch, *Lab Chip*, 2004, **4**, 342–350.
5 Y. Q. Luo and R. N. Zare, *Lab Chip*, 2008, **8**, 1688–1694.
6 E. P. Kartalov, C. Walker, C. R. Taylor, W. F. Anderson and A. Scherer, *Proc. Natl. Acad. Sci. U. S. A.*, 2006, **103**, 12280–12284.
7 B. Mosadegh, C.-H. Kuo, Y.-C. Tung, Y. Torisawa, T. Bersano-Begey and S. Takayama, *Nat. Phys.*, 2010, DOI: 10.1038/NPHYS1637.
8 J. A. Weaver, J. Melin, D. Stark, S. R. Quake and M. A. Horowitz, *Nat. Phys.*, 2010, **6**, 218–223.
9 Y. S. Heo, L. M. Cabrera, J. W. Song, N. Futai, Y. C. Tung, G. D. Smith and S. Takayama, *Anal. Chem.*, 2007, **79**, 1126–1134.
10 B. H. Jo, L. M. Van Lerberghe, K. M. Motsegood and D. J. Beebe, *J. Microelectromech. Syst.*, 2000, **9**, 76–81.
11 J. H. Kang, E. Um and J. K. Park, *J. Micromech. Microeng.*, 2009, **19**.
12 W. R. Childs and R. G. Nuzzo, *J. Am. Chem. Soc.*, 2002, **124**, 13583–13596.
13 A. L. Thangawng, M. A. Swartz, M. R. Glucksberg and R. S. Ruoff, *Small*, 2007, **3**, 132–138.
14 L. Yang, N. Shirahata, G. Saini, F. Zhang, L. Pei, M. C. Asplund, D. G. Kurth, K. Ariga, K. Sautter, T. Nakanishi, V. Smentkowski and M. R. Linford, *Langmuir*, 2009, **25**, 5674–5683.
15 M. A. Eddings, M. A. Johnson and B. K. Gale, *J. Micromech. Microeng.*, 2008, **18**.
16 N. L. Jeon, D. T. Chiu, C. J. Wargo, H. K. Wu, I. S. Choi, J. R. Anderson and G. M. Whitesides, *Biomed. Microdevices*, 2002, **4**, 117–121.
17 A. Mata, E. J. Kim, C. A. Boehm, A. J. Fleischman, G. F. Muschler and S. Roy, *Biomaterials*, 2009, **30**, 4610–4617.
18 B. H. Chueh, D. Huh, C. R. Kyrtsos, T. Houssin, N. Futai and S. Takayama, *Anal. Chem.*, 2007, **79**, 3504–3508.
19 H. K. Wu, B. Huang and R. N. Zare, *Lab Chip*, 2005, **5**, 1393–1398.

